ORIGINAL ARTICLE

Future climate and its impact on streamflow: a case study of the Brahmaputra river basin

Pulendra Dutta[1] · Gilbert Hinge[1] · Jeffrey Denzil K. Marak[1] · Arup Kumar Sarma[1]

Abstract

Using various GCM (general circulation model), the present study attempted to analyze the impact of climate change on the entire stretch of one of the major rivers in South Asia, the Brahmaputra river basin. Initially, we identified a suitable GCM based on some statistical measures of the interpolated and bias-corrected variables. The results of the trend analysis show a significant impact on the climatic variables during future periods. The Brahmaputra basin is likely to experience an increase in rainfall, maximum temperature, and minimum temperature at the rates of 2.5 mm/year, 0.062 °C/year and 0.05 °C/year, respectively, corresponding to representative concentration pathway (RCP) 8.5 scenarios till the end of the current century. Moreover, the climate change impact analysis on streamflow indicates a rise of up to 13.06% in annual discharge at Pandughat, India. The findings of this study will provide a basis for water resource management of the transboundary Brahmaputra basin in the coming decades.

Keywords Brahmaputra · Climate change · Streamflow

Introduction

In recent years, increased concentration of greenhouse gases, notably carbon dioxide, has been reported, which induce climate change around the world (Arrow 2007; Hinge et al. 2018, 2020). This change leads to an increase in the average global temperature, which in turn affects the global hydrological cycle (Pervez and Henebry 2015). Changes in the hydrological cycle are affecting the intensity and duration of precipitation (Trenberth 2011), magnitude of streamflow (Ma et al. 2008), and thereby affect drought and flood (Huntington 2006) characteristics. Thus, the changing climate will have a significant implication on water resource management.

There have been many studies in recent years that assessed the likely impacts of climate change on basin hydrology and water availability (Kim et al. 2008; Pervez and Henebry 2015; Singh and Kumar 2018). All these climate change studies depend on projections of future climate provided by general circulation models (GCM). However, GCM outputs may produce error/biases due to their limited spatial resolution and various thermodynamic as well as climate system processes. Even in cases of regional climate models (RCM), where the climate is simulated by considering the regional characteristics of the area under investigation, there are observed biases between the simulation and the in-situ measurements (Lazoglou et al. 2019). Hence, they cannot directly be used as input to any semi-distributed or lumped hydrological model. Otherwise, the error between the GCM output and the historical observations is often observed to be significant (Ramirez-Villegas et al. 2013). Therefore, the GCM models have to be downscaled to an appropriate, but the higher resolution (Von Storch et al. 1993).

The issues of uncertainties of future climate data of various downscaled GCM outputs are not yet avoidable (Chen et al. 2011). Taking these uncertainties into account along with other factors such as time constraints, human resources, and computational constraints, the downscaling of GCM models is not a straight forward or simple task, especially for a large area like the Brahmaputra river

✉ Gilbert Hinge
  gilberthinge@gmail.com

1 Department of Civil Engineering, Indian Institute of Technology Guwahati, Guwahati, Assam 781039, India

basin (area ≈ 6,00,000 km^2) having numerous observed weather stations. To tackle this problem, one approach may be to adopt the bias-correction coupled with spatial interpolation methods to bring the GCM outputs close to the observed climate variables. The availability of several grid points of GCM within its boundary of a large area, even many of them lying at the proximity of the observed weather stations, justifies the applicability of interpolation and bias correction methods in climate impact studies of the Brahmaputra basin.

The Brahmaputra basin is also known to be of the most vulnerable to climate change because of its diverse climate and topographic variation (Pervez and Henebry 2015). The upper part of this basin receives its discharge from the snow-melt before it enters India (Singh and Kumar 2018). However, once the Brahmaputra enters the Indian state through Arunachal Pradesh, its basin experiences heavy rainfall until it ends the journey at the Bay of Bengal. The river basin hazards like alternation in its channel configuration, sediment transport, and flood are some common phenomena because of high discharge (Goswami 1985) of the Brahmaputra. Despite these facts, not many studies have been carried out in terms of the vulnerability of climate change in the entire basin. There have been numerous case-specific studies (Goswami 1985; Sarma 2005; Akhtar et al. 2011; Ghosh and Dutta 2012; Sahoo and Sreeja 2015) regarding hydrologic, hydraulic, and sediment analyses on the Brahmaputra river. Other case studies (Bongartz et al. 2008; Immerzeel 2008; Mahanta 2014) regarding the climate change impact have noted an increase in the average annual temperature, monthly evaporation, and monthly rainfall. But all these studies were performed for a particular part of the basin, rather than considering the entire basin. As per the author's knowledge, the mighty Brahmaputra basin has been hardly studied as a single unit incorporating the complete river stretch starting from the source at Tibet to the mouth at the Bay of Bengal. Although, Aktar et al. (2015) considered the entire river stretch, the results of this study could not be taken at confidence since the hydrologic model was calibrated for discharge at only one gauge station viz. Bahadurabad, Bangladesh. The change in future streamflow at the same location was also evaluated based on the perturbed values of GCM data (Alam et al. 2016). Here, future rainfall and temperature data were generated by applying some hypothetical factors to analyze the subsequent impact on streamflow. The study carried out by Mohammed et al. (2017) also considered the entire stretch to analyze climate change impact, but for the same location only. None of these studies forwarded the future climate change variability in terms of spatial and temporal analyses throughout the basin. However, the present study is carried out using interpolated and bias corrected data of certain GCMs for spatial and temporal analysis throughout the entire basin.

The present study aims to evaluate the pattern of climate change and its impact on the entire Brahmaputra basin. As the performance of GCMs can vary depending on the location, multiple GCM datasets available at the Earth System Grid Federation were evaluated to identify the most suitable one for the area of interest. First, the output of each GCM was interpolated to the desired weather station location, followed by the bias correction using the historical data. Standard statistical measurements are then used to identify the best performing GCM by comparing its output with the observed data. The bias-corrected outputs of the selected GCM were used to assess the possible impact of climate change on the basin. This impact analysis includes quantification of the variability and trend of the climate variables of the basin in the ongoing century as well as the changes in the hydrological parameter of the basin using a hydrological model in the Soil and Water Assessment Tool (SWAT) platform.

Study area

The present study is carried out for the Brahmaputra River basin (Fig. 1), which covers four different countries, namely China, India, Bhutan, and Bangladesh. The Brahmaputra River originates in Southern Tibet at an elevation of 5300 m. Out of its total length of 2880 km, the Brahmaputra covers a major part of its journey in Tibet and then flows through India to merge into the Bay of Bengal in Bangladesh. China occupies the major part of the basin area (~ 50%), followed by India (~ 36%), and the other two nations, i.e., Bhutan and Bangladesh share almost equally (~ 7%). This river is popularly pronounced as 'Tsangpo' in Tibet; 'YarlungZangbo' in China; 'Siang'/'Brahmaputra' in India and 'Jamuna'/'Meghna' in Bangladesh. The basin is characterized by high spatial variations of topography, land use, and weather variables. This river basin has a wide spatial variation of temperatures that range from negative values at the Himalayan region to 35–39 ^{0}C during summer in the plain areas. Expanding over 5,80,000 square kilometers, this basin experiences a wide spatial variation of rainfall magnitudes that ranges from very low values at the Himalayan region to very high values at the plain.

Data selection

Certain GCM of CMIP5 archive were selected based on their suitability for the Brahmaputra basin and its sub basin as identified in the previous work, and on the availability of data for the present and the future period**.** Previous work carried out by Sarthi et al. (2016) used both IPSL-CM5 and HadGEM-2CC model for their study on Brahmaputra.
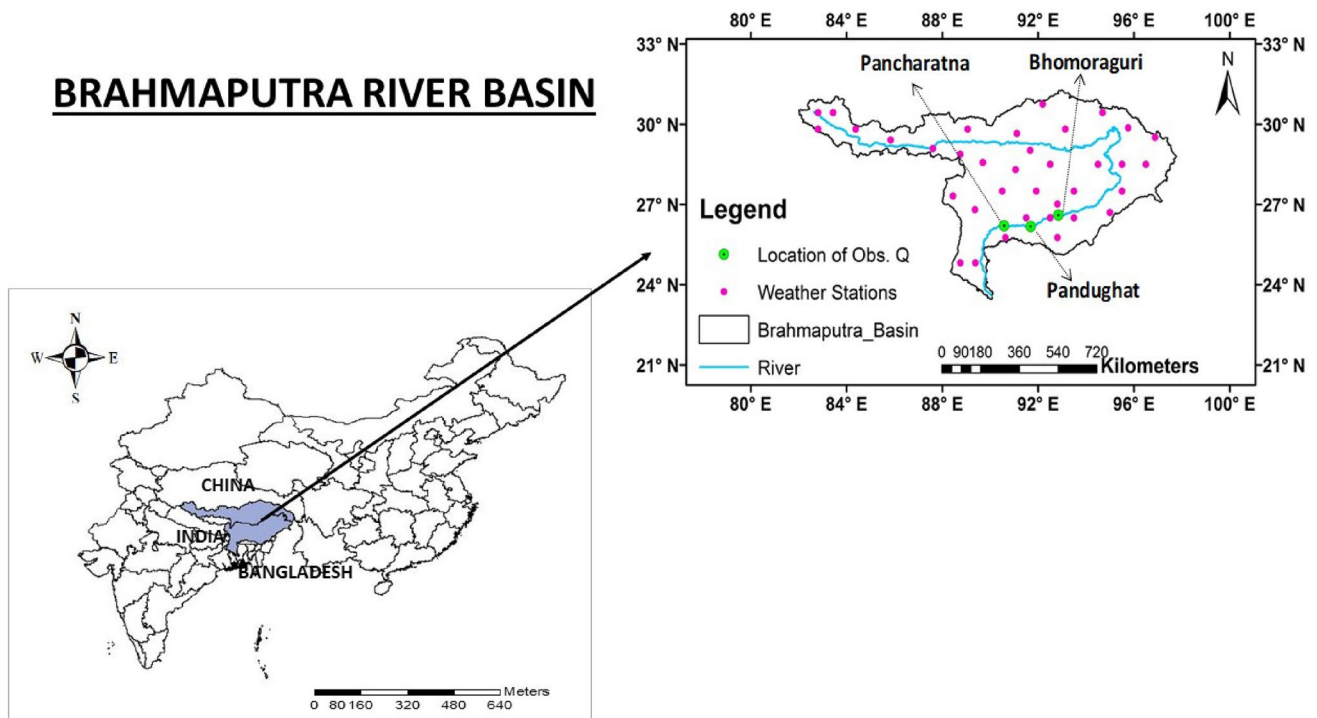
Fig. 1 Study area showing the main river, location of meteorological stations, and location of observed discharge (Q) (Pancharatna, Bhomoraguri, and Pandughat)

Whereas the work carried out by Saharia and Sarma (2018) used the bias-corrected GFDL ESM2M model to evaluate the future climate change impact on hydrological cycle in an area within the Brahmapatra basin. Both these studies proves that these models work well for the Brahmaputra basin and/ or part thereof. The present study involves the complete stretch of the Brahmaputra basin, and, therefore, we selected all the three GCMs mentioned earlier Viz. GFDL-ESM2M, HadGEM2-CC, and IPSL-CM5-1R for the analysis. The grid size of each GCM is presented in Table 1. For our analysis, two RCP (representative concentration pathways) scenarios viz. RCP4.5 and RCP8.5 were chosen to represent the complete range of impact.

Referring to the previous works (Dutta and Sarma 2020), we have selected observed weather data corresponding to three different sources, the combination of which was found the best suitable for analyzing the hydrology over the Brahmaputra basin. These include (i) climate forecast system reanalysis (CFSR) data provided by Texas A&M University; (ii)

IMD (Indian Meteorological Department) gridded data generated by Dr. Balaji Narasimhan, Associate Professor, IIT Madras; (iii) Measured data at certain gauge stations over Tibet (China), obtained through academic collaboration. Out of numerous observed weather stations [(i) + (ii) + (iii)] data, we selected 36 stations (Fig. 2b) data so that at least one station falls within each major sub-basins (Fig.S1), preferably the point near the geometric center. For the present analysis, we utilize three observed variables, namely precipitation (PCP), temperature maximum (TMax), and temperature minimum (TMin) spanning over 15 years (1991–2005) records. Any missing value was filled up by interpolating the corresponding available weather records. Any variable if not available in the later three datasets are copied from the nearest corresponding CFSR dataset. The GCM data corresponding to PCP, TMax, and TMin were obtained for both the historical (1991–2005) as well as future (2006–2099) periods from the Coupled Model Intercomparison Project Phase 5.

Table 1 GCMs used in the present study

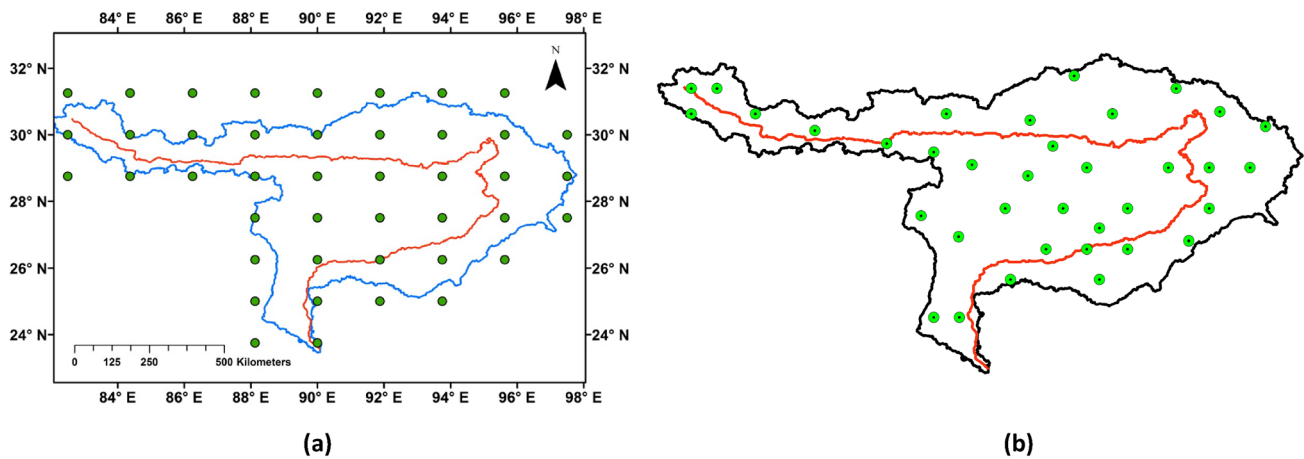| GCM	Grid	Archive
GFDL-ESM2M	$(2.02 \times 1.25)°$	Coupled Model Inter-comparison Project Phase-V (CMIP5)
HadGEM2-CC	$(1.25 \times 1.875)°$	
IPSL-CM5-LR	$(1.89 \times 3.75)°$	

Fig. 2 Weather stations: **a** GCM coordinates (HadGEM2-CC, for example); **b** observed weather stations (36 numbers) considered for climate change studies

Methodology

Interpolation

We have utilized raw data of nine GCM grid points (Fig. 2) for processing, and to obtain interpolated data corresponding to an observed weather location using Inverse Distance Weighted Average (IDWA) interpolation method. The IDWA method is given by the equation (Eq. 1) as follows:

$$V_{\mathrm{f}} = \frac{\sum_{i=1}^{n} \frac{1}{d_i^2} V_i}{\sum_{i=1}^{n} \frac{1}{d_i^2}}, \tag{1}$$

where V_{f} is the interpolated value required at the station, V_i is the data at grid point I; d_i is the distance of i from the station, n is the number of points. Here the power 2 was chosen by evaluating the cross-validation statistics of different power value.

Using Eq. 1, we generated a set of 'interpolated data' for each of the 36 weather locations of three climatic variables viz. PCP, TMax, and TMin. All these interpolated values are then bias-corrected by adopting an appropriate method.

Bias correction

Climatic processes are simulated using the equations of conservation of mass, energy and momentum. These climate models called general circulation models (GCMs) are used for study and prediction of future climate (Singh et al. 2019). The models simulate large-scale processes and it is very difficult to capture minute details that occur on a regional scale. Thus, the outputs of the GCM are bound to have some deviations from the actual data better known as the bias.

Therefore, bias correction of GCM outputs before using it for any hydrological study is of prime importance. In the present analysis, bias correction was carried out, whereas no downscaling was adopted because large numbers (Fig. 2a) of GCM points (~25 nos.) are available within the study area.

Linear scaling method (Teutschbein and Seibert 2013; Shrestha et al. 2017) was employed for bias correction of the interpolated GCM outputs. This method is based on the difference between monthly observed and raw GCM values. These differences are then applied to climate data to obtain bias-corrected climate variables.

$$\text{Bias correction factor} = M_{\mathrm{O}} - M_{\mathrm{G}}, \tag{2}$$

where, M_{O} is the monthly mean observed for a particular month, M_{G} is the monthly mean raw GCM data for the same month as M_{O}.

Additive correction is used for temperature, and multiplicative correction is used for precipitation, as defined by Hempel et al. (2013). Additive correction is used for the temperature to ensure that absolute changes (whether positive or negative) are not modified; however, precipitation being a non-negative parameter, a multiplicative correction is applied to make sure that the corrected data are non-negative.

The following equation, as defined by Shrestha et al. (2017), were used for Linear scaling correction:

$$P_{\mathrm{h}}(d)^b = P_{\mathrm{h}}(d) \times \left[\mu_{\mathrm{m}} \times P_{\mathrm{obs}}(d) / \mu_{\mathrm{m}} \times P_{\mathrm{h}}(d)\right], \tag{3}$$

$$P_{\mathrm{rwf}}(d)^b = P_{\mathrm{rwf}}(d) \times \left[\mu_{\mathrm{m}} \times P_{\mathrm{obs}}(d) / \mu_{\mathrm{m}} \times P_{\mathrm{h}}(d)\right], \tag{4}$$

$$T_{\mathrm{h}}(d)^b = T_{\mathrm{h}}(d) + \left[\mu_{\mathrm{m}} \times T_{\mathrm{obs}}(d) - \mu_{\mathrm{m}} \times T_{\mathrm{h}}(d)\right], \tag{5}$$

$$T_{rwf}(d)^b = T_{rwf}(d) + \left[\mu_m \times T_{obs}(d) - \mu_m \times T_h(d)\right], \qquad (6)$$

here '*P*' refers to precipitation, '*T*' for temperature, '*d*' refers to daily, 'μ'$_m$ refers to the long-term monthly mean, the superscript letter '*b*' refers to bias-corrected, 'h' refers to historical raw GCM data, 'obs' refers to observed data and 'rwf' is the raw GCM future data.

Uncertainty analyses: evaluation of GCMs

Climate change studies are generally forwarded by taking the outputs from several GCMs. The present study considers three GCMs for computation of interpolation followed by the bias correction based on their historical (1991–2005) records. However, managing the GCM data and its processing to make them useful for both the present and future climate change studies are computationally very expensive. It becomes more tedious for the large Brahmaputra river basin considering numerous gauge weather stations. Therefore, the present climate change study for the future periods (2006–2099) is intended to forward by utilizing the outputs of a GCM identified as the best among the selected GCMs. This section describes the evaluations of the performances of all GCMs based on the historical (corrected) records, and to identify one GCM that best replicates the observed weather records. It is assumed that the GCM identified best suitable for the historical records would reflect the same for the future periods too. The most suitable GCM so selected would be considered for future climate change studies.

The ability of the GCMs to simulate the historical PCP, TMax and TMin values can be assessed using a different type of evaluation measure. However, no individual measure is considered superior to the other, instead of combined use of different measures can provide a comprehensive assessment of the model performance (Flato et al. 2014). For this study, the corrected outputs of the GCMs are compared with the observed data using statistical measures defined by the World Meteorological Organization (WMO). These statistical measures include root mean square error (RMSE) [Eq. 7] and Nash–Sutcliff efficiency (NSE) [Eq. 8].

$$RMSE = \sqrt{\frac{1}{N}\sum_{i=1}^{N}(S_i - O_i)^2}, \qquad (7)$$

$$NSE = 1 - \left(\frac{\sum_{i=1}^{n}\left(O_i - S_i\right)^2}{\sum_{i=1}^{n}\left(O_i - \overline{O}\right)^2}\right), \qquad (8)$$

here '*S*' and '*O*' refers to the simulated (i.e., model generated) and observed values, $\overline{O}$ and $\overline{S}$ are the mean of observed and model-generated data series, '*i*' denotes the simulated

and observed pairs, and '*N*' refers to the total number of such pairs.

Trend analysis

To quantify the temporal trends of climate variables across the study area till the year 2099, the present study first used the nonparametric Mann–Kendall test to detect the existence of increasing or decreasing trend (Kendall 1975), then followed by nonparametric Sen's method to estimate the magnitude of the trend (Sen 1968). A two-tail test is performed using a significance level α to evaluate significance increase or decrease of the data set. For this analysis, α is taken as 0.05. Based on this level, the *Z* statistic value (Z_C) greater than 1.96 indicate significant increasing (positive) trend and value Z_C lower than − 1.96 represents significant decreasing(negative) trends, respectively.

The trend analysis is applied to the bias-corrected HadGEM2-CC data during 2020–2099, for both the RCP4.5 and RCP8.5 scenarios. To identify the local trend existing in the long time series, analyses were carried out by dividing the data into smaller timescales, i.e., 2020–2040 (Future1, i.e., "F1"), 2041–2070 (Future2, i.e., "F2") and 2071–2099 (Future3, i.e., F3).

Results and discussion

Bias correction results

Initially, the bias correction factors on a monthly basis are calculated using Eq. 2. These factors are different for different GCMs and different stations. An example is shown in Table S1, indicating the values of bias correction factors. Similar factors are obtained for the weather variables at all other stations, and corresponding to all three GCMs. Here, the correction factors on a monthly basis are assumed to remain constant over the present as well as future periods. Later, these factors are applied to the interpolated (raw) GCM outputs using the respective equations (Eqs. 3–6), to obtain the bias-corrected daily outputs at a station. By principle, the bias factors calculated based on the historical records are assumed to remain the same throughout and, therefore, applicable for the future climatic records too.

Applying the bias factors, we generated a set of data for the bias-corrected climate variables. Figure 3 shows an example of comparison of raw, bias-corrected and the observed daily data for PCP and TMax. Similar results are observed for TMin and even at all the other stations. This is evident from this figure that while correcting for bias, the raw GCM data points which were at far distant from the observed ones became closer to the later. Even a few points, especially during 90–150 days of the year, the bias-corrected
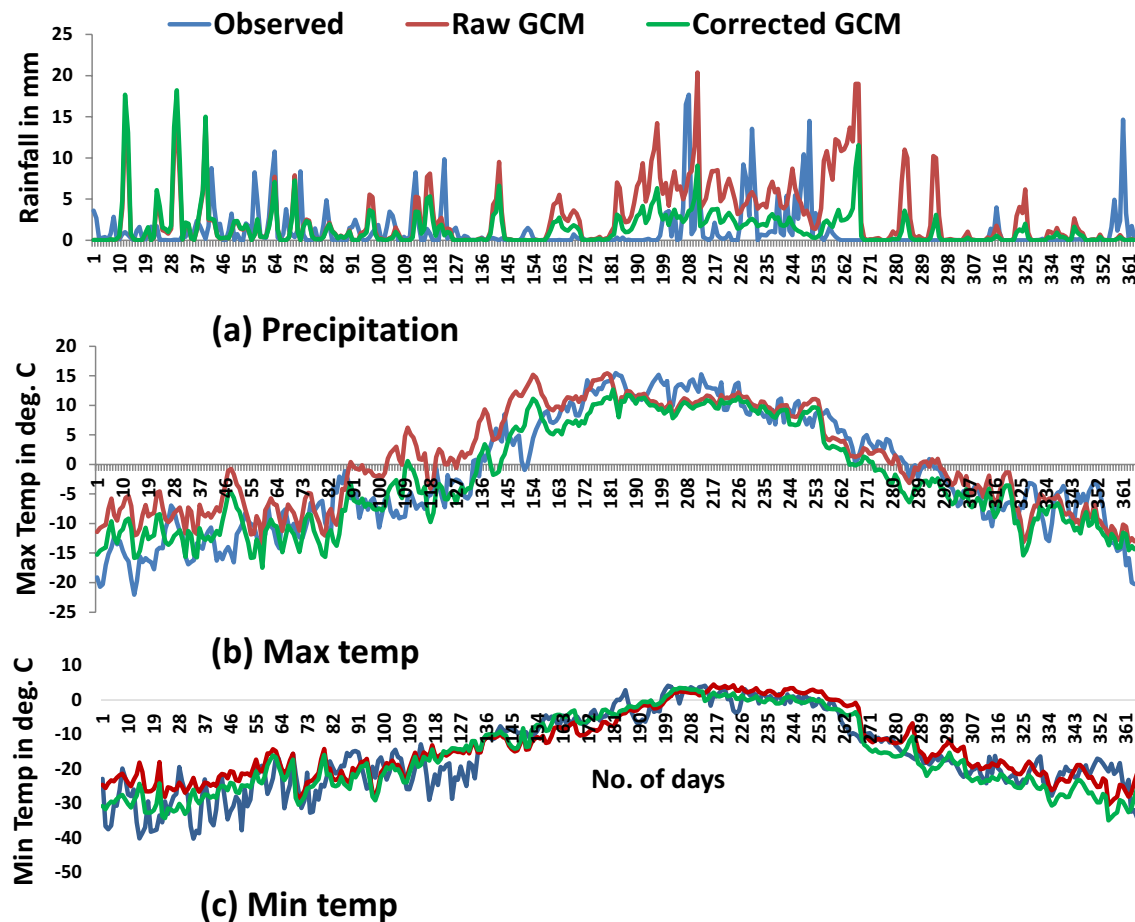
Fig. 3 Values of bias corrected GCMs [for IPSL-CM5-LR] with respect to observed data for 1 year (1991) only, at a station (S1) for **a** precipitation (top) and **b** maximum temperature (bottom) and **c** minimum temperature (bottom)

values are almost concentric to the observed values. It is evident that the raw data after correcting for biases do not exactly tally with the observed values. The bias correction methods are incapable to remove the model biases completely. However, the magnitudes of the raw GCM outputs are brought closer to that of the observed variables at the ground. It is not possible to match the corrected GCM outputs with the observed ones at the point to point scale. This is because the linear scaling method is based on the long term monthly mean values. As such, the monthly mean values of the corrected GCM values become the same as the corresponding observed values.

Figure 4 shows the comparison of the bias-corrected variables with the observed variables on a monthly basis. Rainfall being a non-negative parameter, multiplicative correction is applied to them. On the other hand, the additive correction was applied to the temperature data to ensure absolute changes not being modified. Therefore, the total rainfall in a month remains the same for both the corrected GCM and the observed data sets. For example, the total rainfall corresponding to the corrected GCM (GFDL-ESM2M)

during March at station S5 (Lat: 29.82 N; Long: 89.06 E) is 36 mm that is exactly same in magnitudes as the observed rainfall during the same month. Similar results at the same locations are observed for TMax ($+0.48$ °C) and TMin (-12.9 °C) of GFDL-ESM2M, during the same month. Such kinds of results are also prevalent for the other GCMs viz. IPSL-CM5-LR and HadGEM2-CC, and even at all the weather locations considered in this study. This signifies the monthly values of the bias-corrected GCM variables stand the same as the magnitudes of observed climatic variables. It, therefore, the climate impact studies using input values on a monthly basis provide better results than on a daily basis. So, bias correction provides the reasonably acceptable outputs of the GCM, similar to the observed values, and they might further be utilized for climate change studies of an area.

Selection of GCMs

The data series of all GCMs and the observed records on a daily basis corresponding to each weather station is utilized
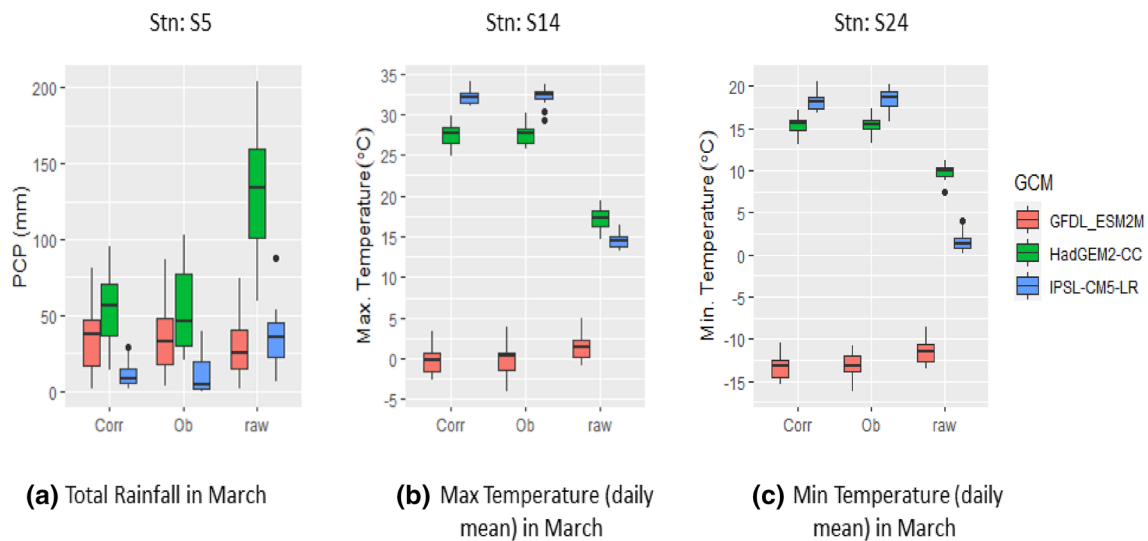
Fig. 4 Box plot for monthly mean values of rainfall, maximum temperature and minimum temperature at certain salient stations selected on a random basis. Here, the GCM outputs are shown for GFDL-ESM2M at station S5 (29.82 N: 89.06 E); for IPSL-CM5-LR at station S14 (26.8 N: 89.36E) for HadGEM2-CC at S24 (26.5 N:92.5 E) for March only

for calculation of the RMSE and NSE. The spatial distribution of RMSE values is shown in Fig. 5. It is evident from the figure (Fig. 5) that all the GCMs simulate rainfall with error in the range of 1–20 mm/day or even more in some stations. The GFDL-ESM2M simulations had errors up to 5 mm/day in the northern region. In the southern and eastern regions, five stations had maximum errors (RMSE > 20). The HadGEM2-CC had error values ranging from 0 to 20. But as compared to GFDL-ESM2M, there were lesser number of stations falling under RMSE > 20 mm/day. It can be seen from Fig. 5 that most of the stations had errors within 0–5 mm/day range. In the case of IPSL-CM5-1R, the error rates were higher in the northern and southeastern regions (> 15 mm/day). On the other hand, the central region had errors within 0–15 mm/day.

The RMSE values of TMax as produced by GFDL-ESM2M ranges from 3.6 to 4.5 °C, in the northern region, whereas the errors are comparatively less in the central region. This error was found maximum in two stations located at the extreme east. In the case of HadGEM2-CC, more errors were prevalent in the central region, with the RMSE range of 3.1° to 4°. The IPSL-CM5-1R performs well in simulating TMax with a lesser number of stations showing 4.1–4.5 range of RMSE. Most of the stations show RMSE under a value of 4. In the simulation of TMin, the GFDL-ESM2M shows the highest error in the most upstream part of the basin (> 4.5). The central region was able to capture the observed values within RMSE values of 2–3, whereas the RMSE was higher in the northeast region of the basin. For the HadGEM2-CC model, many stations have RMSE > 4.1 as compared to the other two GCMs. The stations located in the central regions show higher error

rates. In the case of IPSL-CM5-1R, only four stations were found with RMSE > 4.5. The majority of the stations have RMSE within 2–3, and few stations scattered in the RMSE range of 4.5–4.5. Thus, the spatial variability of the RMSE at each weather station considered across the large Brahmaputra river basin is much significant, thereby leads to difficulty in culminating the performance of GCMs. Therefore, the results of RMSE, as well as the NSE values, are summarized in Table 2.

It can be seen from this table (Table 2) that the HadGEM2-CC performed better than the other two models in simulating mean PCP with RMSE of 9.81 and NSE of −0.04. Likewise, in TMax and TMin as well, the HadGEM2-CC outperformed GFDL-ESM2M and IPSL-CM5-LR. Thus, it becomes evident from the above analyses that the outputs of the bias-corrected HadGEM2-CC provide better agreement to the observed data than that of the other GCMs. As such, this GCM would be utilized for the future climate change studies of the Brahmaputra basin.

Impact analyses due to climate change

The bias-corrected values of the most suitable GCM (i.e., HadGEM2-CC) was forwarded in the climate change impact analyses. Initially, we downloaded the future data (2006–2099) of this GCM only, for the RCP4.5 and RCP8.5 scenarios, followed by interpolation and bias correction. Then, the climate change trends were analyzed using these bias-corrected values of PCP, TMax, and TMin. We considered 1991–2005 as historical and 2006–2099 as the future period. Since the period 2006–2019 has already been over, we carried out Man–Kendall and Sen's slope trend analysis

Fig. 5 RMSE of the GCMs in simulating precipitation (mm/day) (first row), maximum temperature (°C) (second row), and minimum temperature (°C) (third row) at different stations of the Brahmaputra Basin. Different columns refer to different GCMs

for the remaining future period (i.e., 2020–2099) only. However, the bias-corrected data during the period 2006–2019 is used in certain analyses of climate change impact of the Brahmaputra basin.

To evaluate the climate change impact on the discharge of the basin, the study makes use of a hydrological model (Dutta and Sarma 2020) in the Soil and Water Assessment Tool (SWAT) platform. SWAT as a physically based model that simulates the physical processes through the input parameters like topography, land use, climate variables and soil properties (Goyal et al. 2018). The basin boundary is delineated using the SRTM (Shuttle Radar Transmission Mission) Digital Elevation Model (DEM) of 90 m spatial resolution. The stream network is generated for the threshold drainage area of 20,000 km². In SWAT, the Brahmaputra basin watershed is divided into 41 sub-watersheds, which are then further subdivided into 1578 numbers of hydrologic response units (HRUs). The HRUs represent an area consisting of dominant land use, soil characteristics, topography, and management practices. The present study

utilizes MODIS-based landuse of 0.5 km resolution and soil map provided by Food and Agriculture Organization (FAO) at 0.9 km spatial resolution. Incorporating sensitivity and uncertainty analyses of the SWAT model, we applied multi-site calibration and validation for discharge, at three locations (Fig. 1) namely Bhomoraguri, Pandughat, and Pancharatna. Finally, the performance of the hydrologic model was evaluated based on certain statistical parameters like R^2 (coefficient of determination), NS (Nash–Sutcliffe) coefficients etc. The model so established was found to produce a reasonably accepted strength of model outputs (Fig. S5), and could provide a fair replica of the hydrology of the Brahmaputra basin.

Trend analysis result

Fig. S3 describes the trend pattern of changes in maximum temperature at a certain station for RCP4.5 and during the F1 (2020–2040) period, for example. Here, the value in the y-axis, for a year is obtained by averaging

Table 2 Root mean square error (RMSE) and Nash–Sutcliff efficiency (NSE) of precipitation (mm/day), maximum temperature (°C) and minimum temperature (°C) evaluated on three GCMs

Variable	GCM	Indices	Mean	Standard deviation	Max	Min	Median	First quartile	Third quartile
Precipitation	GFDL-ESM2M	RMSE	10.08	7.19	23.38	1.44	7.45	3.83	15.26
		NSE	−0.16	0.21	0.04	−0.87	−0.11	−0.20	−0.02
	HadGEM2-CC	RMSE	**9.81**	**7.17**	24.29	1.39	7.26	3.28	15.37
		NSE	**−0.04**	**0.11**	0.17	−0.34	0	−0.09	0.02
	IPSL-CM5-LR	RMSE	10.64	7.52	26.15	1.49	7.48	4.01	15.96
		NSE	−0.27	0.24	0.09	−0.89	−0.21	−0.40	−0.09
Max. temp (TMax)	GFDL-ESM2M	RMSE	3.75	0.47	4.65	2.78	3.81	3.39	4.07
		NSE	0.48	0.25	0.80	0.05	0.49	0.25	0.70
	HadGEM2-CC	RMSE	**3.33**	**0.39**	4.05	2.47	3.41	2.97	3.81
		NSE	**0.60**	**0.16**	0.83	0.29	0.58	0.46	0.74
	IPSL-CM5-LR	RMSE	3.54	0.39	4.11	2.84	3.63	3.22	3.85
		NSE	0.55	0.22	0.81	0.15	0.56	0.34	0.75
Min. temp (TMin)	GFDL-ESM2M	RMSE	3.38	**0.99**	5.80	2.28	3.17	2.55	3.96
		NSE	0.78	0.06	0.86	0.51	0.80	0.77	0.82
	HadGEM2-CC	RMSE	**3.36**	1.08	5.32	1.84	2.93	2.23	4.06
		NSE	**0.82**	**0.04**	0.88	0.69	0.83	0.81	0.85
	IPSL-CM5-LR	RMSE	3.26	1.06	6.03	2.07	3.08	2.45	3.93
		NSE	0.78	0.17	0.86	−0.19	0.81	0.80	0.83

The best-fitted GCM values are displayed in bold

all days' maximum temperature values during that particular year. In this figure, Z (or Z_c) is the Mann–Kendall statistics, and the trend is said to be 'Significant' (S) if its value is more than 1.96. Otherwise, the trend is 'non-significant' (NS). Moreover, Sen's slope value signifies that the maximum temperature at S26 station during 2040 increases by 4.7% with respect to the base year (2020) corresponding to the RCP4.5 scenario.

Likewise, the trends of all the variables (PCP, TMax, TMin) at all the 36 stations (S1–S36) corresponding to both the scenarios (RCP4.5 and RCP8.5) during all the time scales (F1, F2, F3) are obtained by applying Mann–Kendall and Sen's slope method. Moreover, trend plots are made for the annual and seasonal (i.e., four seasons) changes of climatic parameters. Thus, we have several hundreds of such trend plots for the entire study area. And, we underwent difficulties in presenting such a vast number of trend plots in our report. Therefore, they are presented in the GIS plot, as shown in the subsequent figures, for minimizing the space required in our report and simplicity of presentation. And, the relevant discussions regarding the future climate change of the Brahmaputra basin is forwarded based on the respective figures.

Trends in annual PCP

For the F1 period under RCP4.5, 10 out of 36 stations (Fig. 6) located in the northern part of the basin are found to have significant trends with a moderately high value of Sen's slope. The areas in the southeast of the basin show a significantly increasing trend, whereas the non-significant decreasing trend is seen on the southwestern side. In the F2 period, only two stations in the northern area show a significantly increasing trend. Down the southern areas, a non-significant decreasing trend of PCP is seen. In the late century F3 scenario, the majority of the stations exhibit decreasing trends, and only in the southern areas, one station is found to have an increasing trend.

For the F1 period under RCP8.5, only one station (Fig. 6) shows a significantly increasing trend, and the majority of the stations show a decreasing trend. In the F2 period, the upper half of the basin shows an increasing trend while the lower half shows a decreasing trend. The highest positive values of Sen's slope lie in the upper Indo–China region, and the lowest Sen's slope value lies towards the southern side. Under the F3 period, the areas in the northern side of the basin show a non-significantly decreasing trend, whereas
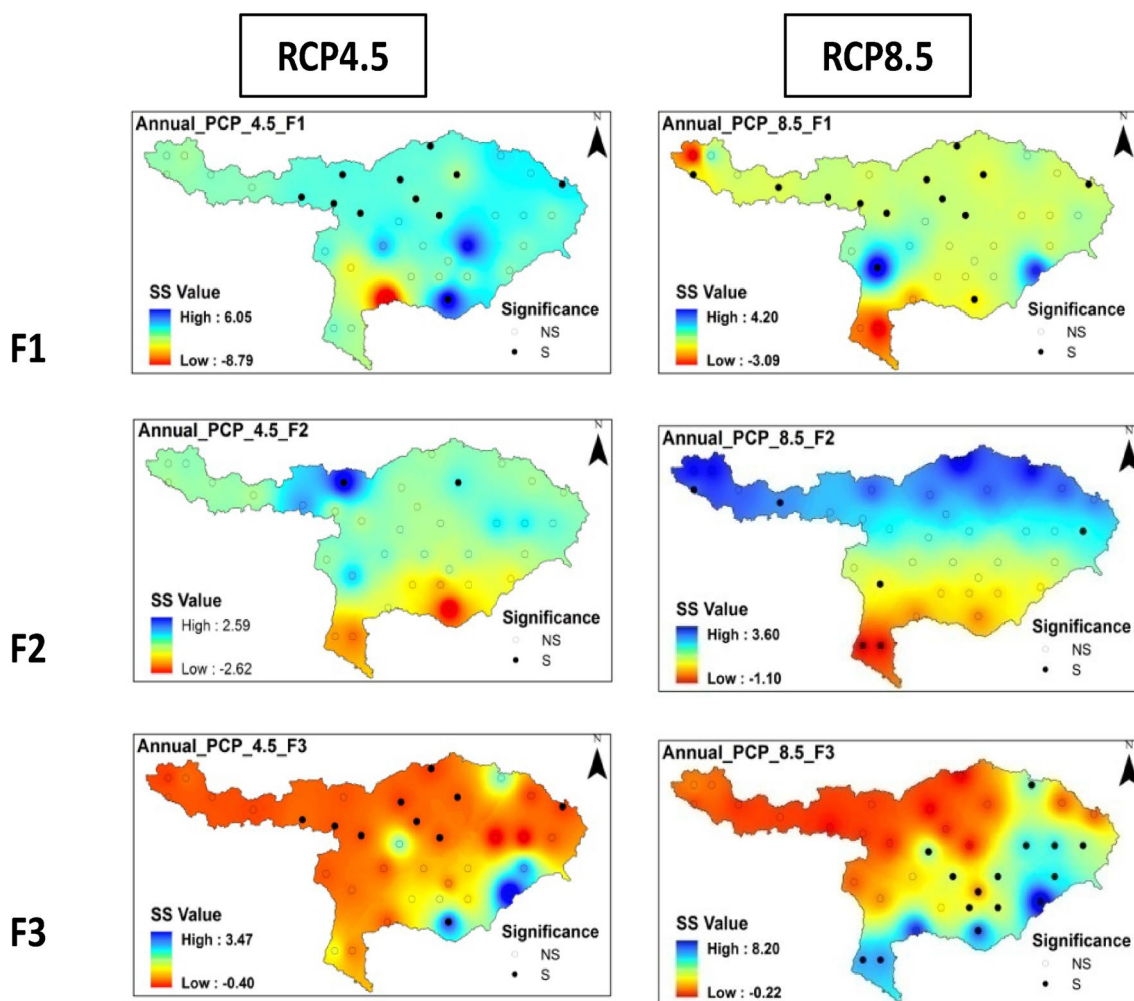
Fig. 6 Simulated (i.e. bias corrected GCM) annual rainfall (PCP) under RCP4.5 (first column) and RCP8.5 (second column) for F1 (2020–2040), F2 (2041–2070) and F3 (2071–2099). Here, the sum of all values of daily rainfall during a particular year over F1 (or F2 or F3) was used for calculation of the Sen's slope (SS) value. Dark circles represent significant (*S*), whereas hollow circles represent non-significant (NS) trend

the southern side of the basin shows increasing trends. The increasing trends were significant in the southern areas of the basin border.

The annual rainfall during 2020–2040 is likely to increase over the majority of the basin areas up to 6.05% (RCP4.5) and 4.2% (RCP8.5). A significant increasing trend in annual rainfall has been observed over the China portion of the basin. This portion is the Himalayan range and would undergo changes in the hydrological cycle due to the increase in rainfall. However, the plain areas over India would experience a relatively low impact in the annual rainfall than the hilly areas. But, the annual rainfall over Bangladesh during 2040 is likely to decrease up to 3.09% with respect to the base year (2020), and corresponding to RCP 8.5. This area of the basin would even undergo shortfall in annual rainfall during 2041–2070. The

Himalayan range would experience a continuous increase in the annual rainfall till 2070, with respect to the base year (2020). Interestingly, this area would suffer a little shortfall in annual rainfall till the end of 2099. But the southern part of the basin is likely to have more impact with an increase in rainfall. During 2071–2099, this change would stand up to + 3.47% (RCP4.5) and + 8.2% (RCP 8.5). While Akhtar et al. (2011) reported an increase of over 5% in annual rainfall in the southern part of the basin. So, the annual rainfall in the Brahmaputra basin would change in the near future following an increasing trend over the majority of the basin areas. However, the snow-fed areas of the Himalayan range and the river mouth portion near the Bay of Bengal would be more susceptible to the future rainfall changes as compared to the plain areas.
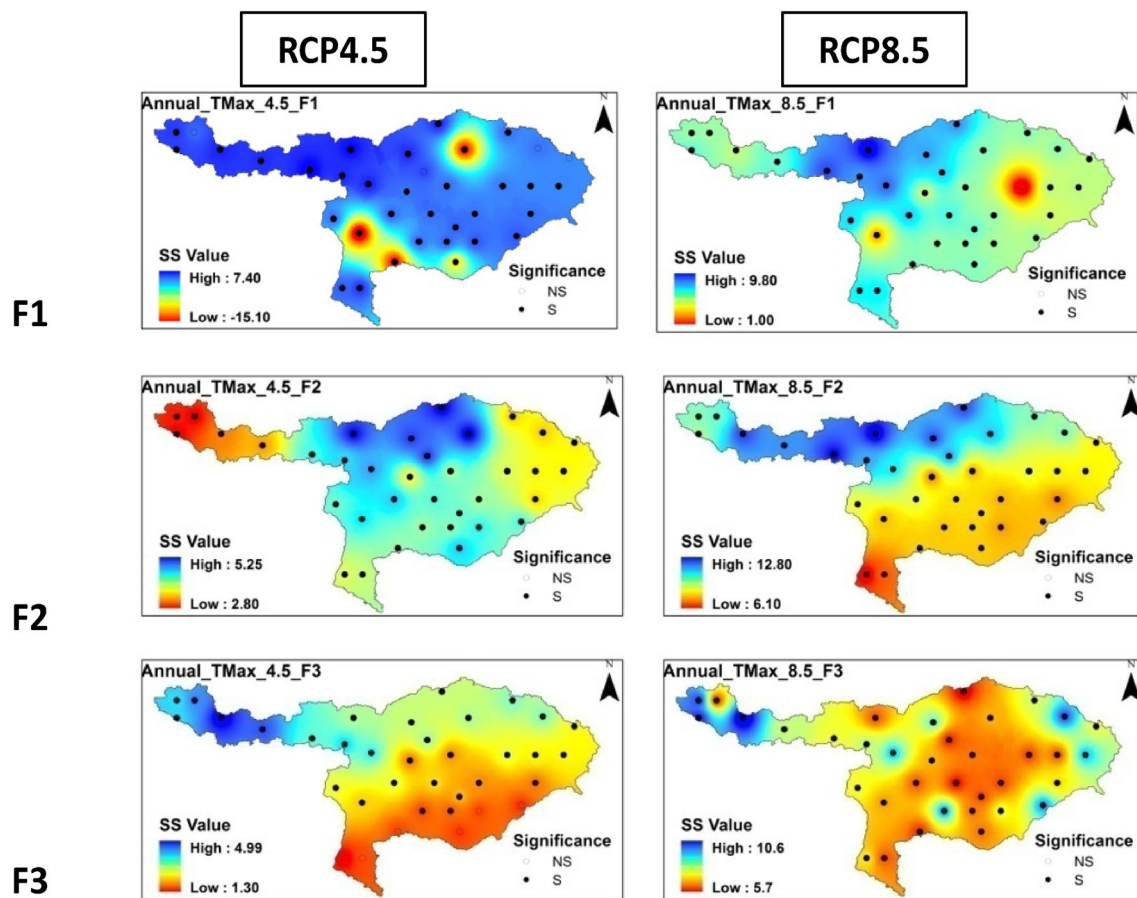
Fig. 7 Simulated (i.e. bias corrected GCM) annual maximum temperature (TMax) under RCP4.5 (first column) and RCP8.5 (second column) for F1 (2020–2040), F2 (2041–2070) and F3 (2071–2099). Here, the average of all values of daily maximum temperature during a particular year over F1 (or F2 or F3) was used for calculation of the Sen's slope (SS) value. Dark circles represent significant (*S*), whereas hollow circles represent non-significant (NS) trends

Trends in annual TMax

The trend analysis of annual TMax for F1 under RCP4.5 (Fig. 7) shows a significantly increasing trend over most parts of the basin with few pockets showing a significantly decreasing trend. The annual maximum temperature may increase up to 7.4% during 2020–2040 which would even escalate up to 8.25% during the next time duration (2041–2070). Of course, the rate of this increase would occur at a relatively slower pitch with maximum value as 4.99% till the end of the century. The plain areas of the basin covering India and Bangladesh would have lesser impacts due to a change in maximum temperature till 2099.

Trend analysis of annual TMax under RCP 8.5 (Fig. 7), the F1 period shows increasing trend all over the basin with Sen's slope ranging from 9.8 to 1. The higher values of Sen's slope are attributed to the northern areas. In F2 period, the increase in TMax is higher (up to 12.8%) in the northern areas whereas an increase in the southern areas would happen up to 6.1%. Moreover, the TMax would increase all over the basin during 2071–2099, with a minimum value of 8.7%.

Comparing RCP4.5 and RCP8.5, it can be seen from Fig. 7 that most of the stations were showing a significantly increasing trend in RCP4.5 with little deviations at a few stations over the study area. But under RCP8.5, all the stations fall under increasing trend with minimum Sen's slope of 1 among all the future periods. Under F2, there is a rise in both upper and lower values of the increasing trend in Tmax for both the RCP scenarios. However, TMax during 2071–2099 would increase at a relatively lower rate, than 2041–2070. Overall, the Brahmaputra basin's annual maximum temperature would increase by the end of the current century.

Trends in annual TMin

For F1 period under RCP4.5 (Fig. 8), the trend analysis of the annual minimum temperature shows the overall increasing trend in the basin with little deviations as decreasing
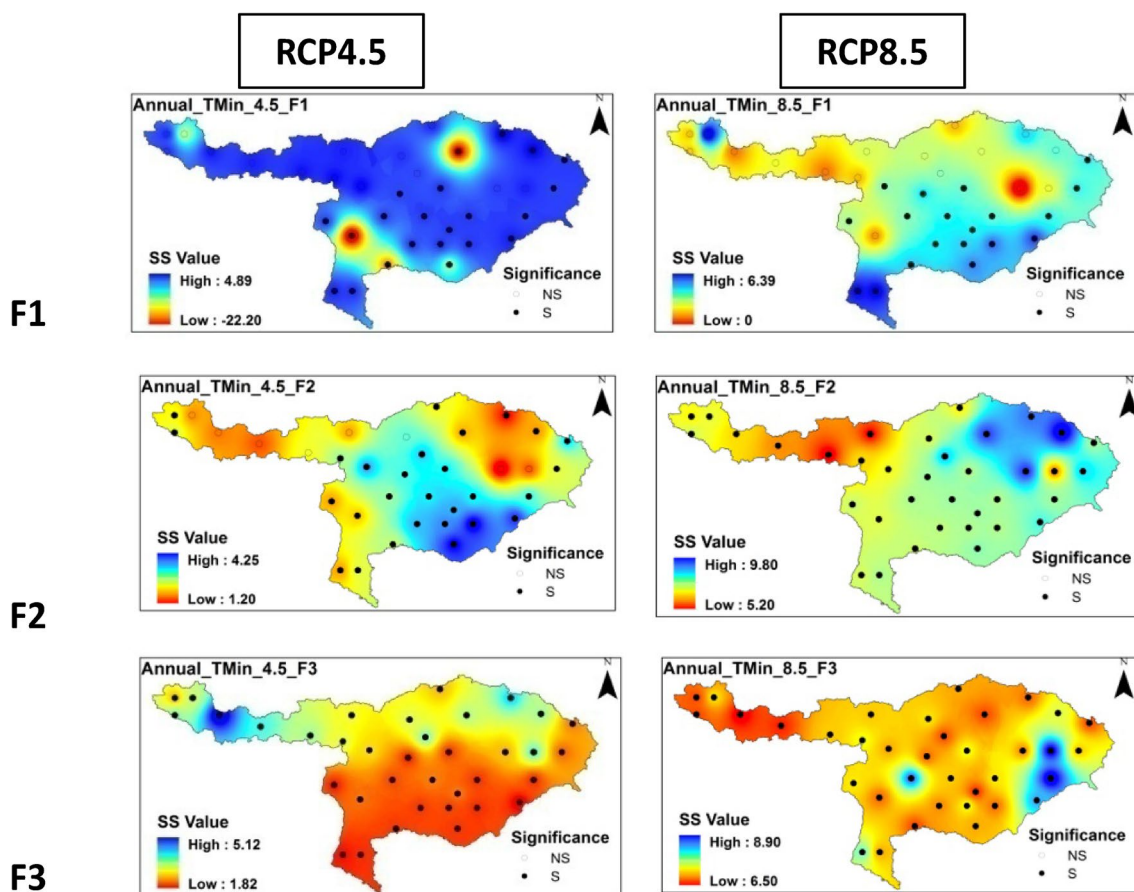
Fig. 8 Simulated (i.e. bias-corrected GCM) annual minimum temperature (TMin) under RCP4.5 (first column) and RCP8.5 (second column) for F1 (2020–2040), F2 (2041–2070), and F3 (2071–2099). Here, the average of all values of daily minimum temperature during a particular year over F1 (or F2 or F3) was used for calculation of the Sen's slope (SS) value. Dark circles represent significant (*S*), whereas hollow circles represent non-significant (NS) trends

trends at only few stations. This deviation perhaps is due to either the incorrect assessment in the GCM outputs or the bias has not been properly removed. The bias factors calculated using the Linear Scaling method is correctly reflected provided the observed records are merely correct that results in correct relationship between these data and the GCM outputs. Moreover, the TMin would increase throughout the basin upto 4.25% for F2 (2041–2070) and 5.12% during F3 (2071–2099). However, the plain areas of India and Bangladesh would have relatively less impact as compared to the hilly areas.

During 2020–2040, the TMin under RCP8.5 (Fig. 8) shows a significantly increasing trend over the plain areas of India and Bangladesh at higher rates than over the northern (China) part of the basin. Here, the maximum increase in TMin would stand up to 6.29%. But, the TMin would even increase at higher rates, over the entire basin during the F2 (2041–2070) period and the value lies in between 5.2 and 9.8%. A similar increasing trend would prevail even during the F3 (2071–2099) period. The TMin would increase up

to 8.5% during 2099 from the base year (2071). Overall, the TMin would significantly increase until the end of the current century.

The annual minimum temperature of the Brahmaputra basin would increase during all the future periods and under both the RCP scenarios. But TMin is likely to decrease at a few stations during 2020–2041 (RCP4.5). This is perhaps not the fair estimate so far the trend values are concerned. Because only two stations, out of 36 total stations considered for climate change analysis is not expected to exhibit the opposite trend than the others, even by a huge margin. Generally speaking, the annual TMin would increase over the entire Brahmaputra basin till 2099, and for both the RCP scenarios.

Annual climate of Brahmaputra basin during 2006–2099

The values of rainfall, maximum temperature, and minimum temperature during 2006–2099 have been plotted in Fig. 9, to understand the pattern of climate change. This
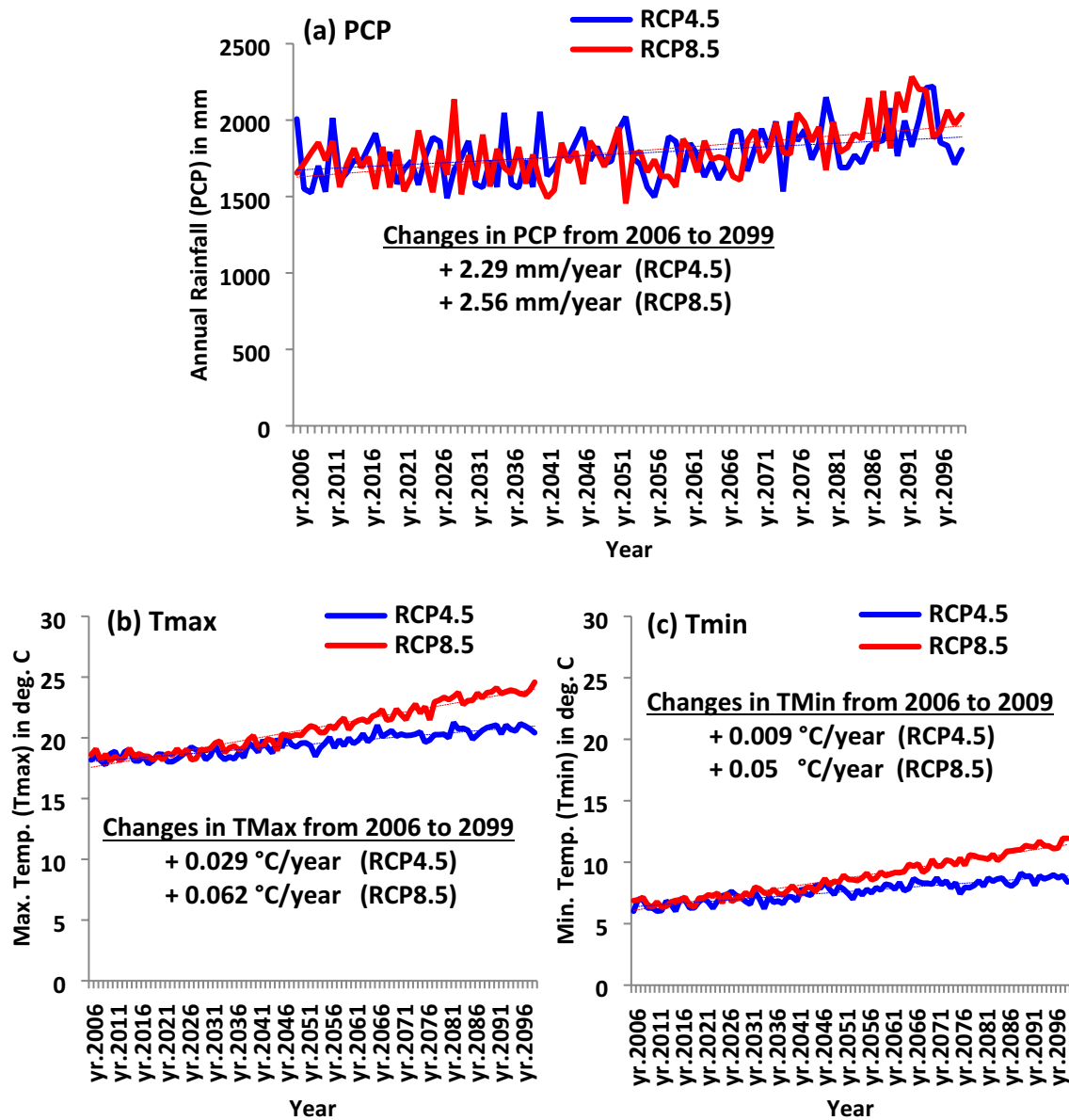
Fig. 9 Pattern of climate changes of the Brahmaputra river basin during 2006 –2099: **a** rainfall (PCP); **b** maximum temperature (Tmax); **c** minimum temperature (Tmin). Here, the blue line corresponds to RCP4.5, and the red line corresponds to RCP8.5

plot shows the basin average values for the interpolated cum bias-corrected climatic variables during the entire period. For precipitation, the daily values in the records of corrected GCM (i.e. HadGEM2-CC) database are added to obtain the total annual rainfall during a particular year. On the other hand, for temperature, the daily values are averaged over a particular year, to obtain the annual temperature value. As per the trend line, the maximum temperature is likely to increase by 3.2 °C (RCP4.5) and 6.8 °C (RCP8.5) starting from the year 2006 to the year 2099. So, the Brahmaputra basin is likely to experience an increase in maximum temperature at the rate of 0.029 °C/year and 0.062 °C/year, for RCP 4.5 and RCP8.5, respectively.

At the end of the century, the minimum temperature of the Brahmaputra basin is likely to increase at the rate of 0.009 °C/year (RCP 4.5) and 0.052 °C/year (RCP8.5), with respect to the base year 2006. Moreover, the annual rainfall of the basin would increase by 2.29 mm/year for RCP4.5, starting from 2006 till 2099. This value stands even higher for RCP8.5, and the value is 2.56 mm/year. So, it is obvious that the climatic variables would increase at higher rates for RCP 8.5, as compared to RCP4.5. It can be concluded from this analysis that the Brahmaputra river basin would experience the impacts of global climate change.

Impact on future discharge

The projected annual discharge time series are divided into three smaller time scale, i.e. from 2020–2040 (F1), 2041–2070, (F2) and 2071–2099 (F3). The discharge values are obtained from the SWAT model run using the bias-corrected GCM (HadGEM2-CC) data for the present as well as for all the future timescales. The annual discharge variability of these three timescales is analyzed and compared with respect to the annual discharge during the base period (2006–2019) of the SWAT model output. The SWAT model is simulated using the daily values of input variables and to provide outputs on an annual basis.

The annual discharge values obtained from the SWAT model simulation for each time scale are shown in Fig. 10, as a box plot. Here, the SWAT model is run using the input variables obtained from the bias-corrected HadGEM2-CC database. The simulation was done for the respective periods (i.e. BP, F1, F2 and F3) individually, and for both the RCP scenarios. Then, the outputs corresponding to three locations (Bhomoraguri, Pandughat, and Pancharatna) are derived from the simulation results for this analysis.

The box-plot result indicates that the mean values of the projected discharge are higher than the base period, for the majority of the timescales under both the RCP4.5

and RCP8.5 scenarios, at all the three locations. From the figure (Fig. 10), it is also evident that there is a wide variation in the maximum discharge values of all the three-time scales at each location with respect to the base period.

Referring to Table 3, which denotes the percentage of changes in annual mean discharges w.r.t. the base period (2006–2019), it has been observed that there is a positive increment, for all scenarios at majority time scales, except few deviations. The basin average annual rainfall (Fig. S4) value during the base period is 1690 mm, for RCP4.5. This value insignificantly changes during the F1 (2020–2040) period. As such, the changes in annual discharge values at all three locations are found to be insignificant. The annual rainfall during F2 period would increase to 1760 mm, thereby the annual discharge value during this period is likely to increase w.r.t. the base period discharge values. Indeed, this is clear from Table 3 that this increase would happen to 4.05% at Pancharatna. However, the annual discharge during F3 period would increase at higher rates, and the values are 8.47% (Bhomoraguri), 9.34% (Pandughat), and 9.93% (Pancharatna). This is due to an increase in annual rainfall to a greater extent (Fig. S4), as a consequence of global climate change. As well, for RCP4.5, the temperature (TMax/TMin) of the Brahmaputra basin during F3 period would increase by 2–3 °C from

Fig. 10 Impact of future climate change on the annual discharges of the Brahmaputra basin at the three locations: **a** Bhomoraguri, **b** Pandughat, and **c** Pancharatna. Here, the results of SWAT model run using bias-corrected HadGEM2-CC corresponding to RCP4.5 and RCP8.5 are shown as box plot
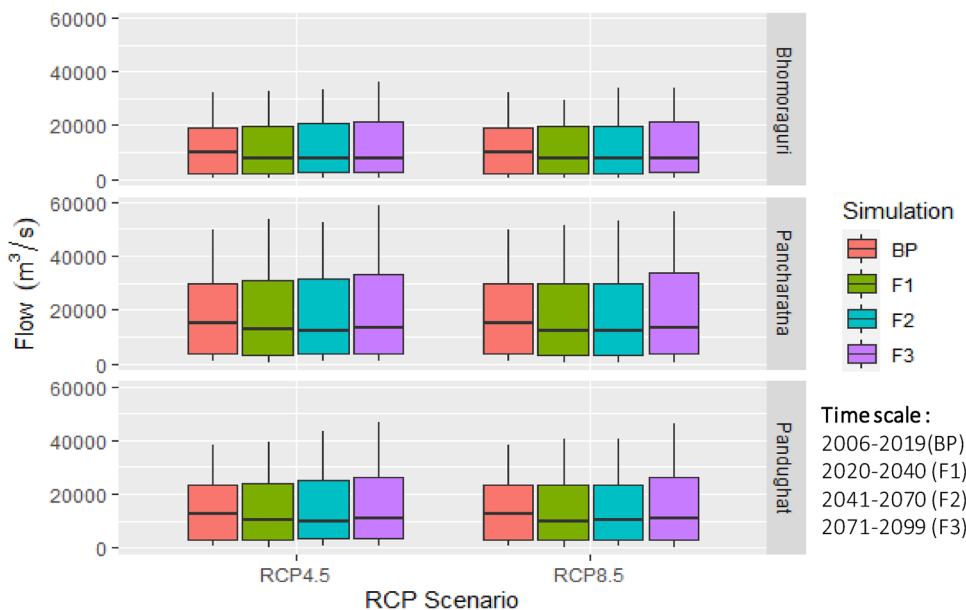
Table 3 Percentage (%) changes in annual discharge due to climate change w.r.t base period (2006–2019)

Location	Future 1 (2020–2040)		Future 2 (2041–2070)		Future 3 (2071–2099)	
	RCP 4.5	RCP 8.5	RCP 4.5	RCP 8.5	RCP 4.5	RCP 8.5
Bhomoraguri	− 1.32	− 3.78	+ 2.75	− 3.36	+ 8.47	+ 3.93
Pandughat	+ 1.25	− 1.50	+ 1.26	− 1.31	+ 9.34	+ 13.06
Pancharatna	+ 0.84	− 1.63	+ 4.05	− 1.63	+ 9.93	+ 12.13

the base period. This would aid to increase in the future annual discharge at the end of the century.

For RCP8.5, the annual discharge during both the F1 and F2 periods would decrease, as compared to the base period. It is evident from Table 3, this decrease may happen up to 3.78%. Of course, the Brahmaputra basin would experience a deficit in annual discharges during F1 and F2 periods, due to the impact of climate change. The annual rainfall values during these periods would decrease, as compared to the base period. However, there is a sharp increase (= 225 mm) in annual rainfall (Fig. S4) over the basin, during F3 periods, w.r.t. the base period. As a result, the Brahmaputra discharge during F3 period would increase to a large extent. The upstream location i.e. Bhomoraguri is likely to have the least impact, whereas the downstream locations (i.e. Pandughat and Pancharatna) are likely to experience relatively greater impact. This is because annual rainfalls during that period are relatively higher in the downstream plain areas than the upstream hilly areas. The highest increase in annual discharge under RCP8.5 would occur at Pandughat (13.06%), followed by Pancharatna (12.13%), during 2071–2099, and with respect to the base periods.

Looking at some of the limitations of this work, the present study used GCMs from three different agencies, which is sufficient to address the model uncertainty, however future study may consider more GCMs or even a multi model ensemble to improve the climate impact assessment. Climate change impact analysis on seasonal variation may also be considered.

Conclusion

Based on the results of interpolation and bias correction, we could identify HadGEM2-CC as the most suitable GCM for the present study area. While comparing the performances of all the GCMs selected in this study, it was observed the data of HadGEM2-CC to replicate merely the ground observations. This information will be helpful to the research community.

Climate change is associated with not only the rise in temperature but also with the change in the global precipitation cycle that leads to variation in spatial and temporal patterns. Due to global climate change, the values of climatic variables across the Brahmaputra basin would change until 2099. As per the highest possible emission scenario (RCP8.5) results, the increases in annual rainfall and maximum temperature of the basin are likely to stand up to 2.56 mm per year and 0.062 °C/year, till the end of the running century. Increasing precipitation may result in an increased flood, whereas the increasing trend of temperature would result in the melting of glaciers over the Himalayan range of the basin area. Subsequently, the Brahmaputra basin would undergo changes in the basin behaviour, due to change in the basin hydrology. The impact analysis of future climate change on the annual discharge of the basin indicates the mean values of the projected discharge are higher than the historical time period for both RCP4.5 and RCP8.5 in all the three observed locations. Such a variation affecting the quantity and quality of available water resources of the Brahmaputra basin would lead to an increase in competition among agriculture, ecosystems, settlements, industry, and energy sectors.

Compliance with ethical standards

Conflict of interest The authors have no conflicts of interest to declare.

References

Akhtar MP, Sharma N, Ojha CSP (2011) Braiding process and bank erosion in the Brahmaputra River. Int J Sediment Res 26:431–444

Aktar MN, Al Hossain BMT, Ahmed T (2015) Climate change impacts on water availability in the Brahmaputra basin. In: 5th international conference on water and flood management

Alam S, Ali MM, Islam Z (2016) Future streamflow of Brahmaputra River basin under synthetic climate change scenarios. J Hydrol Eng 21:5016027

Arrow KJ (2007) Global climate change: a challenge to policy. Econ Voice 4(3)

Bongartz K, Flügel WA, Pechstädt J et al (2008) Analysis of climate change trend and possible impacts in the Upper Brahmaputra River Basin–the BRAHMATWINN Project. In: 13th IWRA world water congress

Chen J, Brissette FP, Leconte R (2011) Uncertainty of downscaling method in quantifying the impact of climate change on hydrology. J Hydrol 401:190–202

Dutta P, Sarma AK (2020) Hydrological modeling as a tool for water resources management of the data-scarce Brahmaputra basin. J Water Clim Change jwc2020186. https://doi.org/10.2166/wcc.2020.186

Flato G, Marotzke J, Abiodun B et al (2014) Evaluation of climate models. Climate change 2013: the physical science basis. Contribution of Working Group I to the Fifth Assessment Report of the Intergovernmental Panel on Climate Change. Cambridge University Press, Cambridge, pp 741–866

Ghosh S, Dutta S (2012) Impact of climate change on flood characteristics in Brahmaputra basin using a macro-scale distributed hydrological model. J earth Syst Sci 121:637–657

Goswami DC (1985) Brahmaputra River, Assam, India: physiography, basin denudation, and channel aggradation. Water Resour Res 21:959–978

Goyal MK, Panchariya VK, Sharma A, Singh V (2018) Comparative assessment of SWAT model performance in two distinct catchments under various DEM scenarios of varying resolution, sources and resampling methods. Water Resour Manag 32:805–825

Hempel S, Frieler K, Warszawski L et al (2013) A trend-preserving bias correction–the ISI-MIP approach, Earth Syst. Dynam 4:219–236

Hinge G, Surampalli RY, Goyal MK (2018) Prediction of soil organic carbon stock using digital mapping approach in humid India. Environ Earth Sci 77:172

Hinge G, Surampalli RY, Goyal MK (2020) Sustainability of carbon storage and sequestration. Sustainability: fundamental and application. Wiley, New York, pp 465–482

Huntington TG (2006) Evidence for intensification of the global water cycle: review and synthesis. J Hydrol 319:83–95

Immerzeel W (2008) Historical trends and future predictions of climate variability in the Brahmaputra basin. Int J Climatol A J R Meteorol Soc 28:243–254

Kendall MG (1975) Rank correlation methods, 4th edn. Charles Griffin, London

Kim U, Kaluarachchi JJ, Smakhtin VU (2008) Climate change impacts on hydrology and water resources of the Upper Blue Nile River Basin, Ethiopia. Iwmi, Colomba

Lazoglou G, Anagnostopoulou C, Skoulikaris C, Tolika K (2019) Bias correction of climate model's precipitation using the copula method and its application in river basin simulation. Water 11:600

Ma Z, Kang S, Zhang L et al (2008) Analysis of impacts of climate variability and human activity on streamflow for a river basin in arid region of northwest China. J Hydrol 352:239–249

Mahanta C (2014) Physical assessment of the Brahmaputra River. Jagriti Prokashony, Dhaka

Mohammed K, Saiful Islam AKM, Tarekul Islam GM et al (2017) Impact of high-end climate change on floods and low flows of the Brahmaputra River. J Hydrol Eng 22:4017041

Pervez MS, Henebry GM (2015) Assessing the impacts of climate and land use and land cover change on the freshwater availability in the Brahmaputra River basin. J Hydrol Reg Stud 3:285–311

Ramirez-Villegas J, Challinor AJ, Thornton PK, Jarvis A (2013) Implications of regional improvement in global climate models for agricultural impact research. Environ Res Lett 8:24018

Sahoo SN, Sreeja P (2015) Development of flood inundation maps and quantification of flood risk in an urban catchment of Brahmaputra River. ASCE-ASME J Risk Uncertain Eng Syst Part A Civ Eng 3:A4015001

Saharia AM, Sarma AK (2018) Future climate change impact evaluation on hydrologic processes in the Bharalu and Basistha basins using SWAT model. Nat Hazards 92(3):1463–1488

Sarma JN (2005) Fluvial process and morphology of the Brahmaputra River in Assam, India. Geomorphology 70:226–256

Sarthi PP, Kumar P, Ghosh S (2016) Possible future rainfall over Gangetic Plains (GP), India, in multi-model simulations of CMIP3 and CMIP5. Theor Appl Climatol 124(3–4):691–701

Sen PK (1968) Estimates of the regression coefficient based on Kendall's Tau. J Am Stat Assoc 63:1379–1389. https://doi.org/10.1080/01621459.1968.10480934

Shrestha M, Acharya SC, Shrestha PK (2017) Bias correction of climate models for hydrological modelling–are simple methods still useful? Meteorol Appl 24:531–539

Singh UK, Kumar B (2018) Climate change impacts on hydrology and water resources of Indian River Basins. Curr World Environ 13:32

Singh V, Sharma A, Goyal MK (2019) Projection of hydro-climatological changes over eastern Himalayan catchment by the evaluation of RegCM4 RCM and CMIP5 GCM models. Hydrol Res 50:117–137

Teutschbein C, Seibert J (2013) Is bias correction of regional climate model (RCM) simulations possible for non-stationary conditions? Hydrol Earth Syst Sci 17:5061–5077

Trenberth KE (2011) Changes in precipitation with climate change. Clim Res 47:123–138

Von Storch H, Zorita E, Cubasch U (1993) Downscaling of global climate change estimates to regional scales: an application to Iberian rainfall in wintertime. J Clim 6:1161–1171

Publisher's Note Springer Nature remains neutral with regard to jurisdictional claims in published maps and institutional affiliations.